

MICROMETEOROID IMPACTS ON SPACECRAFT: CAN ASTEROIDAL AND COMETARY DUST BE DISTINGUISHED?

A. T. Kearsley⁽¹⁾, M.J. Burchell⁽²⁾, M.C. Price⁽²⁾, G.A. Graham⁽¹⁾, P.J. Wozniakiewicz⁽¹⁾, M.J. Cole⁽²⁾

⁽¹⁾*IARC, Department of Mineralogy, The Natural History Museum, London, SW7 5BD, UK
Email: antk@nhm.ac.uk*

⁽²⁾*Centre for Astrophysics and Planetary Sciences, School of Physical Science,
University of Kent, Canterbury, CT2 7NH, UK*

ABSTRACT

Both cometary and asteroidal sources should contribute to the population of micrometeoroids (MM) reaching Earth [1,2], although there is debate as to their relative numbers. Small impact features on spacecraft surfaces returned from low Earth orbit (LEO) can provide sufficient evidence to distinguish some, but certainly not all, impacts from these dust sources. In this paper we review the difficulties in attributing a source to MM impactors.

1. INTRODUCTION

Scanning electron microscopy (SEM) and X-ray microanalysis of surfaces returned from spacecraft such as the Long Duration Exposure Facility (LDEF) [3,4], Mir [5] and the Hubble Space Telescope (HST) [6] have yielded information about the composition of particles responsible for hypervelocity impact damage in LEO, although detailed interpretation may be difficult [7]. As well as recognition of impactor origin (space debris or MM [8]), interpretation of size, and measurement of fluxes, it has been possible to interpret a wide range of elemental assemblages. In the case of MM residues, these can be compared to natural silicate, sulfide and metallic materials in chondrite meteorites and other extraterrestrial materials [9], (Tab. 1).

For interpretation of particle origins we need to know:

- 1) Are there diagnostic compositional signatures that can be used to separate cometary MM from asteroidal MM?
- 2) Do cometary MM differ from asteroidal MM in diagnostic particle structure?
- 3) Do the diagnostic compositional or structural signatures survive the violent impact capture process?
- 4) Can laboratory experimental and numerical simulations reproduce the style of impact structure and compositional alteration sufficiently well to provide useful analogues?

Until very recently, it has not been possible to define the unique characteristics of cometary dust by reference to samples collected from a known source. In

the light of new discoveries from two comets (81P/Wild 2 [10] and 26P/Grigg-Skjellerup [11]), laboratory impact experiments by particles with a wide range of composition and internal structure [12,13], and new numerical simulations, we discuss the characteristics of impact residues on spacecraft in LEO, and whether they allow us to recognize sufficient structural and compositional properties of the impactor to determine its origin as cometary or asteroidal dust.

2. SAMPLING AND ANALYSIS

Collection has usually employed one of three methods:

- 1) In-flight analysis of particle mass, velocity (sometimes trajectory) and elemental composition by sophisticated ionization detectors e.g. [14]. Although these systems may yield elemental ratios, they do not reveal mineralogy, textures, or particle structure.
- 2) Examination of exposed spacecraft surfaces returned to Earth from LEO e.g. [15,7]. Time of impact, velocity and vector are usually not known, and the substrate may cause high pressure and temperature shock processing of the impactor. The coarse particle structure may be reflected in the shape of the impact feature, and some materials may survive intact, although they may be difficult to distinguish against the substrate.
- 3) Deployment of collectors designed to capture, preserve and return samples e.g. [16], preferably with the least possible damage, giving opportunity for post-flight analysis by modern laboratory instrumentation.

In this paper we concentrate on the largest data set, the opportunistic collection of materials on non-dedicated surfaces (2, above).

Although earlier workers reported impact residue difficult to find in many craters, the advent of automated fast X-ray mapping techniques now makes location and analysis relatively easy and quick [7]. Many LEO impact structures and residues appear very similar in shape, surface texture and composition to those from light gas gun shots (LGG) [17] of well-

characterised mineral and meteorite powders, despite being formed under velocity regimes substantially beyond the laboratory conditions so far achieved with appropriate analogue impactors (e.g. 6.1 kms^{-1} for simulations of the Stardust comet Wild 2 encounter [18]). The orbital parameters of asteroidal dust streams [19] suggest that impact velocity on encounter with a spacecraft in LEO is likely to lie between 20 kms^{-1} and 40 kms^{-1} [20,21]. The range of potential relative velocity is even greater for dust derived from comets (with the diverse orbital parameters of different families resulting in relative velocity between 10 and $\sim 70 \text{ kms}^{-1}$ [22]). The peak shock pressure suffered by silicate mineral projectiles impacting at $\sim 6 \text{ kms}^{-1}$ is $\sim 90 \text{ GPa}$, resulting in partial melting, but analysis of experimental impact residues reveals little compositional change, although sulfide minerals undergo partial dissociation [12]. At the higher velocity of LEO MM, impact pressures may reach hundreds of GPa with concomitantly greater alteration, including loss of volatile components as vapour.

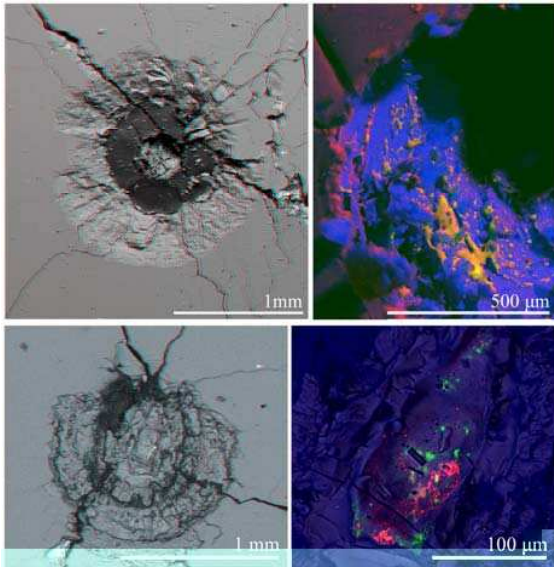


Figure 1. MM impacts on HST solar cells. Stereo SEM anaglyphs (left), X-ray maps (right) of: (top) SM-3B 27.F8 (O red, Si blue Fe green), the splashed residue shows an element ratio similar to that of an olivine with intermediate Mg:Fe ratio; (bottom) oblique impact SM-1 S165 (Si blue, Mg green, Fe red), the assemblage includes Fe Ni metal, Fe sulfide, Fe Ni phosphide, Cr-rich Fe oxide and Mg-olivine.

Larger dust impacts from LEO (Figs. 1,2) may contain distinctive residues, similar to mineral compositions found in laboratory impacts of carbonaceous chondrite meteorite powders (Fig. 3). Are these asteroid or cometary dust impacts?

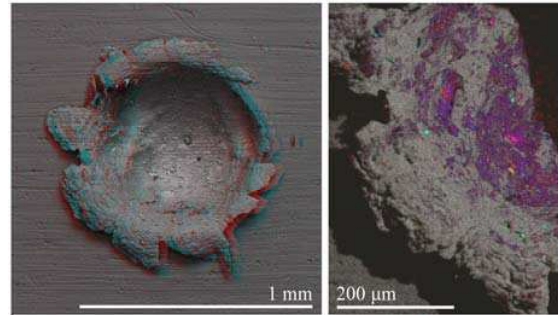


Figure 2. MM impact on LDEF Al clamp EO6 circlip 4: (left) SEM stereo anaglyph, note the complex sub-surface shape; (right) X-ray maps of the left side of the crater: Al grey, Mg green, Si blue, S purple, Ca yellow, Fe red. Element combinations are very similar to those of: Fe, Fe Ni, Fe Cu sulfides; Fe oxide; Ca carbonate; Mg-olivine; Mg-pyroxene; and (possibly) a mixture of serpentine and tochilinite. The assemblage is similar to that found in some carbonaceous chondrite meteorites.

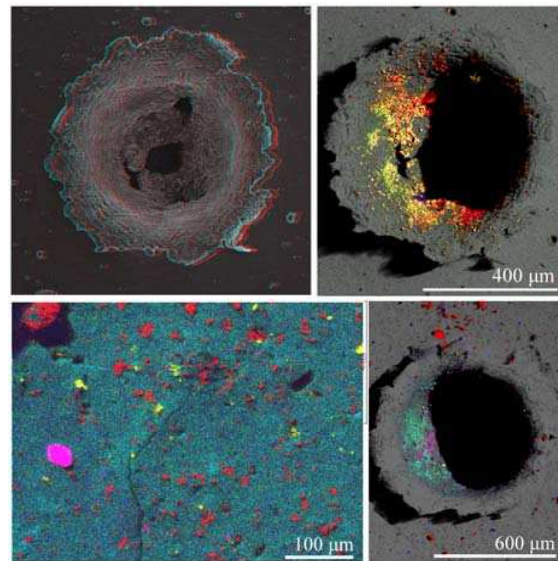


Figure 3. LGG impacts ($\sim 6 \text{ kms}^{-1}$) by meteorite powders: (top) Allende CV3: (left) SEM stereo anaglyph; (right) X-ray maps, Al grey, Mg green, Si blue, S purple, Fe red; (bottom) Orgueil CII X-ray maps of projectile material at left, residue within impact crater at right: Al grey, Mg green, Si blue, S purple, Ca yellow, Fe red.

3. METEOROID AND MICROMETEOROID PROPERTIES: ASTEROID VS. COMET

Several sources of extraterrestrial material are available for laboratory examination and analysis to give 'ground-truth' reference data for the likely compositional and structural characteristics of MM,

which we present as a simplified summary in Tab. 1: meteorites; Antarctic micrometeorites (AMM) and stratospheric collections of interplanetary dust particles (IDPs); as well as samples returned by spacecraft. The inventory of recovered meteorites is now enormous, with many thousands recovered to date, mainly from hot desert and Antarctic ice collections. Their diverse compositions and textures [23] reveal sources from both primitive and evolved parent bodies. For the vast majority there is no detailed information as to when they fell or of their orbit prior to fall (they are described as ‘finds’). Comparison of the spectroscopic reflectance properties from bulk meteorite samples and their individual mineral components to those of specific classes of putative asteroidal parent bodies has provided a number of good matches e.g. [24], although spectral reflectance properties of some asteroid surfaces appear to have been modified by exposure to prolonged micrometeoroid impact and irradiation by energetic cosmic rays [25]. It appears that we have samples of a fairly diverse range of asteroids within the meteorite collections, although biased in numbers towards those which have slower terrestrial weathering rates, and especially to the ordinary chondrites whose parent body orbits currently deliver abundant materials to Earth [26]. Fireball camera networks have now established the orbits of a few recovered ‘fall’ meteorites and have proven that these samples are indeed from bodies with orbits intersecting the main asteroid belt e.g. [27,28]. There is even a suggestion that one very primitive meteorite (the CI carbonaceous chondrite Orgueil, rich in hydrous minerals), may have had an orbit like that of a Jupiter family comet [29]. A great deal is now known about AMM [30,31] which give us samples of fine (sub-mm) particles that have deposited in ice following their entry into the atmosphere. Many particles show evidence of extensive ablation and melting during high velocity atmospheric entry, and the lack of very precise information as to the timing of their arrival prevents attribution to a particular source. Nevertheless, they probably encompass both asteroidal [32] and cometary materials. IDPs again contain a diverse range of small particles [33,34], including some fine-grained and porous clusters of sub-micrometre grains, dominated by anhydrous minerals formed at high temperatures, such as Mg-rich olivine and pyroxene [35], and with peculiar amorphous “glass with embedded metal and sulfides” (GEMS). Although there is still some discussion about their origin, the current consensus suggests that these particles are very primitive, and have not been processed by incorporation into a parent body where heating might allow their compositional alteration. Most researchers regard these anhydrous porous IDPs as samples of cometary dust, and the recent collection of abundant examples containing abundant presolar grains, following the passage of

Earth through the dust tail of comet Grigg-Skjellerup in 2003 [36] seems to confirm this conclusion. Other IDPs are less porous and more dense [37], and show evidence of probable asteroidal origins [38].

Most of the materials in Tab. 1 can be found in all the extraterrestrial settings, although in each different location there may be a distinctive if subtle compositional signature, e.g. the range of olivine compositions in the Wild 2 dust indicates affinity with some carbonaceous chondrite meteorites, yet the lack of easily recognized phyllosilicates suggests that this comet is not similar to the Ivuna-type (CI) carbonaceous chondrites. Although mixing with the target material during impact may make some components (especially fine and amorphous material) difficult to recognize [7], clear differences can occasionally be seen, e.g. Stardust residues from particles < 5 μm in size show a different compositional assemblage to those on HST solar cells (Fig. 4). The greatest difference lies in abundance of sulfide residue, both as sole component within a crater or mixed with silicates. This is unlikely to be purely an artefact of more extensive alteration of very fine sulfides in aggregates (although this may be partly responsible) as there is no evidence of increased metallic droplet abundance, a known by-product of sulfur loss [12]. The HST assemblage is thus probably not from the same particle population as the Stardust cometary collection.

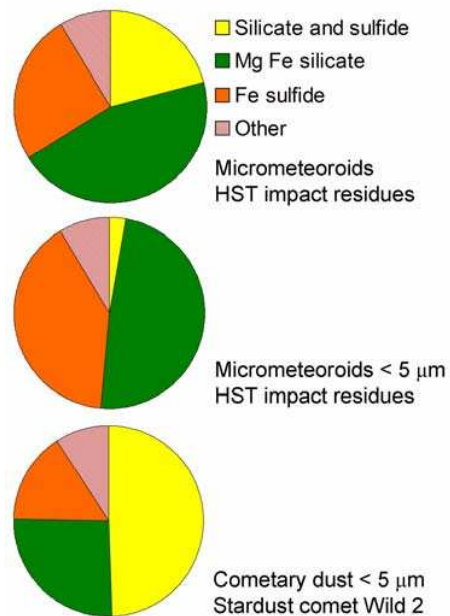


Figure 4. Proportions of MM impact residue types: (top) in craters of all sizes up to 4.5 mm on HST solar cells [9,39]; (middle) craters formed by particles < 5 μm on HST solar cells [9,39]; (bottom) small Stardust craters, formed by particles < 5 μm [40].

Table 1. Comparison of components in chondritic meteorites [23], dust from known cometary sources [41, 11, 42], and LEO impact residues e.g. [3,9]. NYR indicates not yet recognized from this setting, * indicates uncertainty due to problems of preservation, ? indicates possible but not certain attribution.

Material	Composition	[23] Chondritic meteorites (especially CI, CM, CR, CV)	[41] Comet 81P/Wild 2 impacts onto aerogel/foil	[11] Comet Grigg-Skjellerup IDPs	[42] Comet Tempel 1 remote spectroscopy	[3,9] LEO impact residues
Olivine	(Mg,Fe) ₂ SiO ₄	Yes, diverse	Yes, diverse	Yes	Yes	Common
Pyroxene	(Mg,Fe,Ca)SiO ₃	Yes, diverse	Yes, diverse	Yes	Yes	Yes
Hydrous mafic phyllosilicates	Hydrous Mg,Fe silicate	Absent most, but dominates some	NYR*	NYR	Yes?	Yes?*
Feldspar	(Na,Ca)(AlSi) ₄ O ₈	Common	Occasional	NYR	Yes	Yes?
Hibonite	CaAl ₁₂ O ₁₉	occasional	Occasional	NYR	NYR	NYR
Fe sulfide	~ Fe ₇₋₈ S ₈	Common	Common	Yes	Yes	Common
FeNi sulfide	FeNiS	Common, but not in all types	Rare*	Yes	Probable	Common
FeNi metal	FeNi	Common in most	Common*	Yes	NYR	Common
Schreibersite	FeNi ₃ P	Occasional	Occasional	NYR	NYR	Rare
Fe oxides	Fe ₃ O ₄	Common in some	Occasional	NYR	NYR	NYR
Mg/Fe Spinel	(MgFe)Al ₂ O ₄	Common in many	Rare	NYR	NYR	NYR
Cr spinel	(Mg,Fe)(Cr,Al) ₂ O ₄	Common	Occasional	NYR	NYR	Rare
Ca carbonate	CaCO ₃	Absent most, common in some (CM, CI)	Rare	Yes	Yes?	Rare
Amorphous	Mg, Si, Fe, O	Rare, only in some (CR)	Common* but artefact?	Abundant	Inferred	NYR*
Organic		Widespread in carbonaceous chondrites	Yes	Yes	Yes	NYR*
Presolar grains	SiC, diamond, silicates	Rare, except some (e.g. CM)	Rare*	Abundant	NYR	Rare*
Structure		compact	compact	porous	NYR	compact?
Porosity	for most grains	CC 20-30 %	most < 25%?	20-30 %	NYR	low?
Density(gcm ⁻³)	for most grains	1.6 – 3 (gcm ⁻³)	~2.4 (gcm ⁻³)	0.6-1.7(gcm ⁻³)	NYR	2-2.4 (gcm ⁻³)

4. COMETARY DUST COMPOSITION AS REVEALED BY STARDUST

Until very recently, it has not been possible to make direct comparison with materials of undoubted cometary origin. The successful return of the NASA/JPL Caltech Stardust mission [10] has now provided the first assemblage from a known cometary body. A surprising array of materials were revealed, both embedded within the primary collection medium (low density silica aerogel) and within craters on aluminium (Al) foils [43,40]. To help calibrate the aerogel track and Al foil crater sizes, we performed an extensive suite of impacts using the Canterbury LGG [17], operated under the same velocity and incidence conditions as the cometary encounter (perpendicular, at 6.1 kms⁻¹). As well as sub-spherical glass, polymer and metal beads of known size, we used carefully analysed mineral and meteorite powders to act as realistic

compositional analogues [13]. This enabled us to recognise important compositional and textural artefacts from the capture process, and to study track and crater morphology created by projectiles of known properties. The bulk chemical composition of Wild 2 is similar to that of Ivuna-type (CI) carbonaceous chondritic meteorites [44]. However, this Jupiter family comet appears to be dominated by relatively

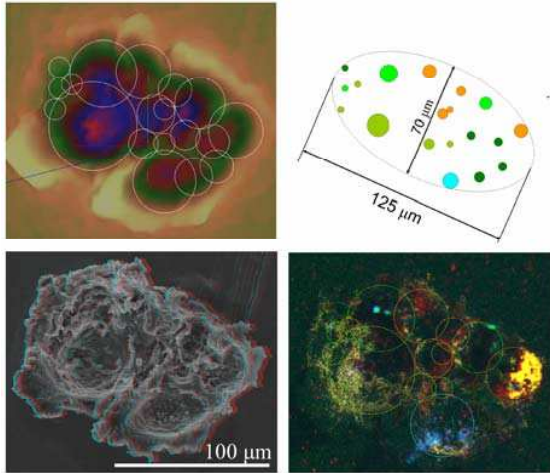


Figure 5. Stardust foil C029W,1. Impact by an unusual, large porous aggregate particle from comet Wild 2. The complex crater is shown in: (top left) a depth model with superimposed overlapping sub-crater rims as white rings; (bottom left) SEM stereo-pair anaglyph; (bottom right) X-ray maps for Mg (green), Si (blue), S (yellow), Ca (purple), Fe (red); (top right) a simple model of the inferred internal structure, used to generate the AUTODYN model of Fig. 6.

5. DUST STRUCTURE AND THE SHAPE OF IMPACT STRUCTURES ON METAL

It now seems that residue composition alone will not resolve the origin of impacting MMs. Can we use crater shape to recognize, for example, impacts by very porous and low density grains such as those suggested to be cometary [47]? Crater shape has been shown to reflect properties of the impactor e.g. [48,49], and our mineral and aggregate particle impact experiments [13] have demonstrated the control exerted by particle density and shape. As the grain-size, bulk density and porosity of many types of meteorites and IDPs are now known [50,37], we have been able to make comparisons to Wild 2 cometary dust [51].

With the development of software for the reconstruction of three-dimensional shape from SEM images [13], we can now quantify shape of even very small impact features. Like the features on the LDEF Al clamp in Fig. 2, the majority of Stardust foil craters are relatively deep compared to width, similar to features produced by single mineral grains or large dense aggregates (but not lower-density smaller aggregates) in our LGG experiments [13]. Laboratory impacts of single dense mineral grains under Stardust encounter conditions yield impact craters that are simple in profile, and are easily distinguished from the complex, shallow and broad features that we have also recently produced using realistic analogues of lower density porous dust aggregates [51], and which are

responsible for features such as that in Fig. 5. The experimental shots have now replicated the entire range of Stardust crater forms, and most of the aerogel track features, giving us confidence in our models of cometary dust particle structure [51]. Many of these features are also very similar to those produced by impact of carbonaceous chondrite powders. Together, these give density values for Wild 2 aggregate particles of 2.4 g cm^{-3} or greater, similar to [48,52] derived from LEO impact data. In Wild 2, very fine-grained, very porous aggregates of low density, un-equilibrated and rich in amorphous and pre-solar grains, postulated to be abundant in very primitive outer solar system bodies [47], seem to be relatively rare (despite their presence in IDPs attributed to cometary origin).

However, to make comparison to LEO, we still face the difficulty of extrapolating particle impact behaviour to the LEO encounter velocities. Do the differences in crater shape as a function of particle characteristics persist into higher velocity regimes? At the moment, we cannot reach the necessary conditions in laboratory experiments, and have begun a series of numerical simulations using AUTODYN, initially to compare directly to craters generated in our LGG experiments (for validation) and simulate Stardust craters of varying complexity (Fig. 6). It has been suggested [48] that crater depth/diameter (D_e/D_i) is effectively invariant for velocities $> 5 \text{ km s}^{-1}$, but our first results suggest that this may not be the case (Fig. 7). We intend to extend simulations of both simple grains and complex aggregate impacts into a range of higher velocities, appropriate for LEO impact of MM. These should provide us with a realistic 'identity parade' of diagnostic crater morphology, show how velocity influences complex impact feature excavation, and show how easy or difficult it may be to distinguish impacts from high and low-porosity particles in velocity regimes appropriate for Earth orbits.

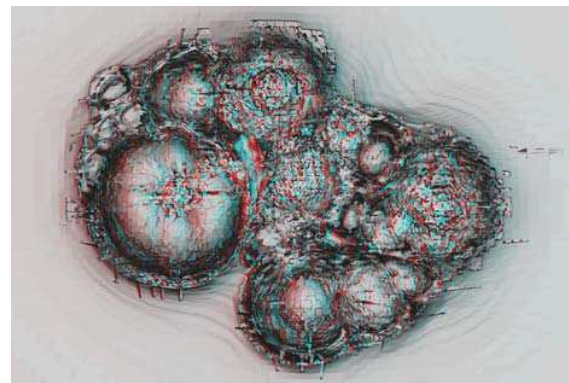
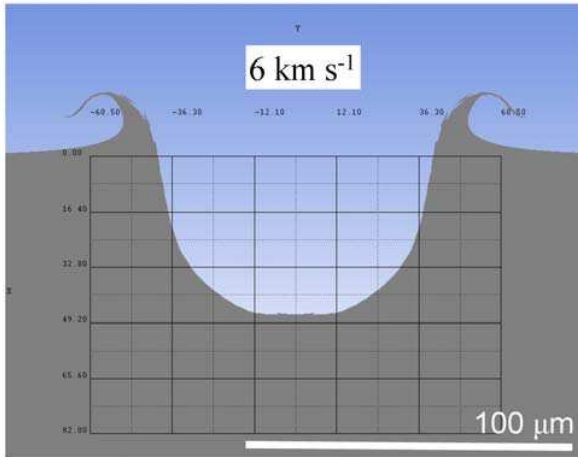


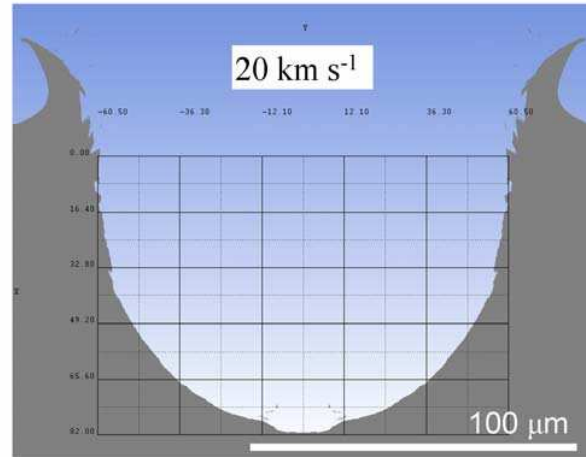
Figure. 6. Stereo anaglyph snapshot from an AUTODYN 3D simulation of the complex Stardust impact feature in Fig. 5. Uplift of septa, by interference between growing internal crater bowls, is in progress.



$$De/Di = 47.6 \mu\text{m} / 82.3 \mu\text{m} = 0.58$$

$$\text{Crater inner diameter} = \text{projectile} \times 3.6$$

$$\text{Crater top lip diameter} \approx \text{projectile} \times 4.8$$



$$De/Di = 82 \mu\text{m} / 121 \mu\text{m} = 0.68$$

$$\text{Crater inner diameter} = \text{projectile} \times 5.3$$

$$\text{Crater top lip diameter} \approx \text{projectile} \times 7.4$$

Figure 7. AUTODYN 2D models of impact of soda-lime glass spheres (22.8 micrometres diameter) on aluminium Al1100 alloy at 6 km s^{-1} and 20 km s^{-1} , note increased Depth/Diameter (De/Di) at the higher velocity.

6. CONCLUSIONS

MM residues and crater shapes can be used to determine the composition and structure of the particles responsible for impacts on spacecraft surfaces, and do demonstrate differences between samples. Whether individual particles can be shown to come from an asteroidal or cometary source is much more of a problem and the composition of MM residue is not a reliable way to distinguish asteroidal and cometary dust. Even when it is possible to disentangle the effects of high shock pressures and temperatures associated with particle capture on the most gentle of capture substrates, we now know that the recovered particles are usually the most robust components, which may be very similar in both asteroidal and cometary dust. The common components of MM residues require extensive preparation before more subtle and diagnostic compositions can be found. The samples from Wild 2 suggest that the composition of solid materials in comets and many asteroids may be so similar as to be indistinguishable. The shape of impact features on spacecraft suggests most were formed by relatively dense grains, which might have been assumed to be asteroidal, but again Wild 2 shows that cometary dust can be dominated by micrometre-scale and coarser grains, with density similar to that of carbonaceous chondrite meteorites. So far, there have not been large numbers of reports of very shallow or complex craters which might be expected from low-density, highly-porous cometary dust particles such as those collected in IDPs from Grigg-Skjellerup.

If one can make unambiguous measurements of orbital information for small impactors, will it be possible to recognise the origin of individual impactors? This would require careful integration of active time, velocity and trajectory sensors e.g. [53] with a gentle particle capture cell that can be returned intact to Earth for extensive laboratory examination and analysis. However, the discovery of intermittent cometary behaviour in some asteroids (e.g. members of the Themis family with spectroscopic properties of C-type [54] within the outer part of the Main Asteroid Belt), suggests that even when orbital dynamics have been resolved, materials from these two classes of small bodies may not be clearly distinguishable.

7. REFERENCES

1. Ipatov, S.I. et al. (2008). Dynamical zodiacal cloud models constrained by high resolution spectroscopy of the zodiacal light. *Icarus* **194**, 769–788.
2. Jenniskens, P. (2007) Meteor showers from broken comets. In “Dust in Planetary Systems” (Eds. H. Krueger and A. Graps). ESA SP-643, ESA Publications Division, European Space Agency, Noordwijk, The Netherlands, pp. 3-6.
3. Bernhard, R. P. et al. (1993a). Projectile compositions and modal frequencies on the “Chemistry of micrometeorites” LDEF experiment. In *LDEF-69 months in space, Part 2*. (Ed. A.S. Levine,.) NASA Conference publication 3194, National Aeronautics and Space Administration, Washington, D.C., USA, pp. 551-574.

4. Brownlee, D.E. et al. (1993). Interplanetary meteoroid debris in LDEF metal craters. In *LDEF-69 months in space, Part 2*. (Ed. A.S Levine,.), NASA Conference publication 3194, National Aeronautics and Space Administration, Washington, D.C., USA, pp. 577-584,
5. Hörz, F. et al. (2000). Impact features and projectile residue in aerogel exposed on MIR. *Icarus*, **147**, 559–579.
6. Moussi, A. et al. (2005). Results of the HST solar arrays impact analysis. In Proc. 4th European Conf. Space Debris (Ed. D. Danesy), ESA SP-587, ESA Publications Division, The European Space Agency, Darmstadt, German, pp. 207-214.
7. Graham, G.A et al. (2001). Analysis of Impact Residues on Spacecraft Surfaces: Possibilities and Problems. In Proc. 3rd European Conf. Space Debris, ESA SP-473, ESA Publications Division, The European Space Agency, Darmstadt, Germany, pp. 197-203.
8. Kearsley, A.T. et al. (2005). Impacts on Hubble Space Telescope solar arrays: discrimination between natural and man-made particles. *Adv. Space Res.*, **35**, 1254-1262.
9. Kearsley, A.T. et al. (2006). The chemical composition of micrometeoroids impacting upon the solar arrays of the Hubble Space Telescope. *Adv. Space Res.*, **39**, 590-604.
10. Brownlee, D.E. et al. (2006). Comet 81P/Wild 2 under a microscope. *Science*, **304**, 1711 – 1716,
11. Nakamura-Messenger, K. et al. (2008). Mineralogy of interplanetary dust particles from the comet Grigg-Skjellerup dust stream collections. 71st Annual Meteoritical Society Meeting abstract #5247.
12. Kearsley, A.T. et al. (2007). Analytical scanning and transmission electron microscopy of laboratory impacts on Stardust aluminium foils: interpreting impact crater morphology and the composition of impact residues. *Meteoritics Planet. Sci.*, **42**, 191 – 210.
13. Kearsley, A.T. et al. (2008). Micro-craters in Aluminum Foils on NASA's Stardust Spacecraft: Implications for dust particles emanating from Comet Wild 2. *Int. J. Impact Eng.*, **35**, 1616-1624.
14. Grün, E. et al. (2005). Dust Astronomy, *Icarus*, **174**, 1–14.
15. Bernhard, R.P. et al. (1993b). Scanning Electron Microscope/Energy Dispersive X-ray analysis of impact residues in LDEF tray clamps. In *LDEF-69 months in space, Part 2*. (Ed. A.S Levine), NASA Conference publication 3194, National Aeronautics and Space Administration, Washington, D.C., USA, 541–549.
16. Burchell, M.J. et al. (2006). Cosmic dust collection in aerogel. *Annual Rev. Earth and Planetary Sci.*, **34**, 385 – 418.
17. Burchell, M.J. et al. (1999) Hypervelocity impact studies using the 2 MV Van de Graaff dust accelerator and two stage light-gas gun of the University of Kent at Canterbury. *Meas. Sci. and Technology*, **10**, 41–50.
18. Brownlee, D. E. et al. (2003). Stardust: Comet and interstellar dust sample return mission. *J. Geophys. Res.*, **108(E10)**, 8111.
19. Vokrouhlický, D. et al. (2008). Evolution of dust trails into bands. *Astrophys. J.*, **672**, 696-712.
20. Janches, D. et al. (2003). On the geocentric micrometeor velocity distribution *J. Geophys. Res.*, **108(A6)**, 1222, doi:10.1029/2002JA009789.
21. Drolshagen, G. et al. (2008). Comparison of Meteoroid Flux Models for Near Earth Space. *Earth Moon Planet*, **102**, 191–197.
22. Weissman, P. R. (2007). The cometary impactor flux at the Earth. In Proc. IAU Symposium No. 236 “Near Earth Objects, Our Celestial Neighbors: Opportunity and Risk” (Eds. A. Milani et al.), Cambridge University Press, Cambridge, UK, pp. 441-450.
23. Papike J. J. (Ed.) (1998) *Planetary Materials* Min. Soc. America, Reviews in Mineralogy, **36**.
24. Gaffey, M.J. et al. 2002. Mineralogy of Asteroids. In *Asteroids III*. (Eds. W. F. Bottke Jr. et al.), University of Arizona Press, Tucson, AZ, PP 183-204.
25. Lazzarin, M. et al. (2006). Space weathering in the main asteroid belt: the big picture,” *Astrophys. J.*, **647**, 179–182.
26. Mothé-Diniz, T. and Nesvorný, D. (2008). Visible spectroscopy of extremely young asteroid families. *Astron. & Astrophys.*, **486**, L9–L12.
27. Brown P. et al. (1994). The orbit and atmospheric trajectory of the Peekskill meteorite from video records. *Nature*, **367**, 624-626.
28. Spurný, P. et al. (2003). Photographic observations of Neuschwanstein, a second meteorite from the orbit of the Příbram chondrite. *Nature*, **423**, 151-153.
29. Gounelle M. et al. (2006). The orbit and atmospheric trajectory of the Orgueil meteorite from historical records. *Meteoritics Planet. Sci.*, **41**, 135-150.
30. Kurat, G. et al. (1994). Petrology and Geochemistry of Antarctic micrometeorites,” *Geochim. Cosmochim. Acta*, **58**, 3879–3904.
31. Taylor S. et al. (2007). Size distribution of Antarctic micrometeorites. In “Dust in Planetary Systems” (Eds. H. Krueger and A. Graps). ESA SP-643, ESA Publications Division, European Space Agency, Noordwijk, The Netherlands, 145-148.
32. Genge, M. J. (2008). Koronis asteroid dust within Antarctic ice. *Geology*, **36**, 687–690.

33. Bradley J. P. (2004). Interplanetary dust particles. in "Treatise of Geochemistry" Vol. 1, (Eds. A.M. Davis et al.). Elsevier, Amsterdam, The Netherlands, pp. 689-711.
34. Rietmeijer, F.J.M. (1998). Interplanetary dust particles. In "Planetary Materials" (Ed. J.J. Papike), Min. Soc. America, Reviews in Mineralogy, **36**, Chapter 2, pp. 1-95.
35. Zolensky, M. E. and Barrett, R. (1994). Olivine and pyroxene compositions of chondritic interplanetary dust particles. In "Analysis of Interplanetary Dust." (Eds. M. E. Zolensky, et al.), AIP Conference Proceedings 310. American Institute of Physics, New York, 105-114.
36. Nguyen, A. N. et al. (2007). Remarkably high abundance of presolar grains in interplanetary dust particles collected from the comet Grigg-Skjellerup dust stream. LPSC, 38, CD-ROM, abstract #2332.
37. Joswiak, D. J. et al. (2007). Densities and mineralogy of cometary and asteroidal Interplanetary dust particles collected in the stratosphere. In "Dust in Planetary Systems" (Eds. H. Krueger and A. Graps). ESA SP-643, ESA Publications Division, European Space Agency, Noordwijk, The Netherlands, 141-144.
38. Bradley, J. P. and Brownlee, D. E. (1991) An interplanetary dust particle linked directly to type CM chondrites and an asteroidal origin. *Science*, **251**, 549-552.
39. Kearsley, A.T. (2004). Technical Note 3 - Analysis of Impact Residues on SM-3B HST Solar Arrays. Post Flight Impact Analysis of HST Solar Arrays – 2002 Retrieval. Report to the European Space Agency, Contract No. 16283/02/NL/LvH, UniSpaceKent and Natural History Museum, 62pp.
40. Kearsley, A. T. et al. (2008). Dust from comet Wild 2: Interpreting particle size, shape, structure and composition from impact features on the Stardust aluminium foils. *Meteoritics Planet. Sci.*, **43**, 41 – 74.
41. Zolensky, M. E. et al. (2006). Mineralogy and Petrology of Comet Wild 2 Nucleus Samples. *Science*, **314**, 1735-1739
42. Lisse, C. M. et al., (2006). Spitzer spectral observations of deep impact ejecta. *Science*, **313**, 635-640, 2006.
43. Hörz, F. et al. (2006). Impact features on Stardust: Implications for comet 81P/Wild 2 dust. *Science*, **314**, 1716 – 1719.
44. Flynn, G. et al. (2006) Elemental Compositions of comet 81P/Wild 2 samples collected by Stardust," *Science*, **314**, 1731-1735.
45. Zolensky, M. et al. (2008). Comparing Wild 2 particles to chondrites and IDPs. *Meteoritics Planet. Sci.*, **43**, 261 – 272.
46. Ishii, H. et al. (2008). Comparison of 81P/Wild 2 Dust with Interplanetary Dust from Comets," *Science*, **319**, 447 – 450.
47. Greenberg, J. M., et al. (1989). The interstellar dust model of comet dust constrained by 3.4 μm and 10 μm emission. *Adv. Space Res.*, 9.3, 3-11.
48. Love, S. G. et al. (1995). Morphology of meteoroid and debris impact craters formed in soft metal targets on the LDEF satellite. *Int. J. Impact Eng.*, **16**, 405-18.
49. Burchell, M.J. and MacKay, N. (1998). Crater ellipticity in hypervelocity impact on metals. *J. Geophys. Res.*, **103E**, 22761-22774.
50. Consolmagno, G. J. et al. (2008). The significance of meteorite density and porosity. *Chem. der Erde Geochem.*, **68**, 1-29.
51. Kearsley, A. T. et al. Interpretation of Wild 2 dust fine structure: comparison of Stardust aluminium foil craters to the three-dimensional shape of experimental impacts by artificial aggregate particles and meteorite powders, unpublished.
52. McDonnell, J.A.M. and Gardner, D.J. (1998). Meteoroid morphology and densities: decoding satellite impact data. *Icarus*, **133**, 25-35.
53. Srama, R. et al. (2009). Sample return of interstellar matter (SARIM). *Exp. Astron.*, **23**, 303-328.
54. Hsieh, H. H. et al. Albedos of Main-Belt Comets 133P/Elst-Pizarro and 176P/LINEAR. *Astrophys. J.*, in press.